DOI: 10.1002/zaac.200800220

One-pot Preparation, Spectroscopic and Structural Characterization of Mercury(II) Complexes of Bulky Diimines with Halides and Pseudohalides

Leonardo C. Ferreira[a], Carlos A. L. Filgueiras[a,*], Lorenzo C. Visentin[a], Jairo Bordinhão[a,†], and Manfredo Hörner[b]

[a] Rio de Janeiro / Brazil, Instituto de Química, Universidade Federal do Rio de Janeiro
[b] Santa Maria / Brazil, Departamento de Química, Universidade Federal de Santa Maria

Received April 30th, 2008; accepted May 27th, 2008.

Abstract. The preparation and characterization of two novel $HgCl_2$ and $Hg(SCN)_2$ complexes with bis[N-(2-*tert*-butylphenyl)imine]acenaphthene is here described. One-pot reaction techniques were used, leading to high yields of 75 % and 81 %, respectively. The complexes were characterized by microanalysis, i.r. and ^{1}HNMR spectroscopy, and by single crystal X-ray diffraction. The structures of the complexes present similar characteristics, the most outstanding being the formation of dimers via intermolecular interaction. Whereas the $HgCl_2$ complex shows a unidimensional network due to strong π−π interactions, its $Hg(SCN)_2$ counterpart displays a supramolecular arrangement resulting from non classical hydrogen bond formation.

Keywords: Mercury; α-Diimines; Crystal structures; π-π Interactions; Hydrogen bonds

Introduction

Coordination chemistry involving ligands with 1,4-diazabutadiene groups has attracted much attention in recent years. One of the main reasons for this interest is related to their application as pre-catalysts in olefin polymerization, after this behavior was demonstrated in 1990 by *Brookhart* and collaborators [1]. The first complexes to be used were cationic α-diimine Ni^{II} species, which are effective in ethylene polymerization, as well as in homo- and copolymerization of polar monomers. In 1995 Pd^{II} complexes with bulky diimines were shown to be more active than with smaller ligands [2]. In view of the great success earned by Ni^{II} and Pd^{II} diimine complexes, several other metal ions have also been studied in this respect. Ions such as Zn^{II}, Cu^{II} and Co^{II}, for instance, were proven to be active in polymerization processes [3].

The choice of the diimine is doubtlessly one of the most important items for the catalysis to proceed well. This is linked directly to the substituents on the aromatic rings present in the diimine. The preparation of the ligands is a well-known procedure. Routes for their synthesis have been developed by *Dieck* and *Dietrich* [4], *Fukuda* et al. [5] and *Elsevier* et al. [6]. The most widely used method involves the reaction of 1 equivalent of a dicetone with 2 equivalents of an aniline, catalyzed by a Lewis acid such as formic acid. Several solvents are used, the most common being MeOH and HCO_2H. The reactions lead to high yields and the products can be characterized by C,H,N analysis, i.r. and ^{1}H and ^{13}CNMR, as well as X-ray diffraction.

In most cases the α-diimines are first prepared, characterized and then put to react with the chosen metal salt. It is, however, possible to obtain the final complex in a single stage, by means of the so-called "one-pot reaction". In 2002, *Rausch* et al. [7] succeeded in establishing this synthetic route. 1 equivalent of both acenaphthenequinone and $NiBr_2$ were reacted with 2 equivalents of 2-tert-butylaniline, in the presence of HOAc as solvent and catalyst. The product was isolated and characterized, leading to a 77 % yield of the desired complex, establishing the route as a successful one. After a literature search, only one paper was found describing the preparation and characterization of a Hg^{II} complex with an α-diimine containing a acenaphthene ring [8].

The present paper describes the synthesis and spectroscopic as well as structural characterization of two novel Hg^{II} complexes containing *bis*[N-(2-*tert*-butylphenyl)-imine]acenaphthene. The structure of the ligand has already been reported by us [9].

Results and Discussion

The i.r. spectra of **1** and **2** show the appearance of the characteristic diimine CN stretching vibrations [10]. When Cl is replaced by SCN in the complex, the diimine vibrations occur at 1666(ν_{as}) and 1626(ν_s) cm^{-1}, respectively. Comparing these values with those of the free ligand, which are observed at 1664(ν_{as}) and 1640(ν_s) cm^{-1}, respectively,

* Prof. C. A. L. Filgueiras
Instituto de Química
Universidade Federal do Rio de Janeiro
C.P. 68563
21945-970 Rio de Janeiro / Brazil
Tel.: 55-21-2562-7812; fax: 55-21-2562-7559
E-mail address: calf@iq.ufrj.br

Table 1 Crystal data and structure refinement for **1** and **2**

Empirical formula	$C_{32}H_{32}Cl_2N_2Hg$(**1**)	$C_{32}H_{32}N_4S_2Hg$(**2**)
Formula weight	716.12	761.35
T /K	295(2)	295(2)
Radiation, λ /Å	0.71073	0.71073
Crystal System, space group	*triclinic*, $P\bar{1}$	*monoclinic*, $P2_1/c$
Unit cell dimensions, *a*, *b*, *c* /Å	a = 11.5395(3)	a = 11.3839(2)
	b = 12.4890(3)	b = 22.5820(4)
	c = 12.7860(3)	c = 12.4162(2)
	α = 65.5190(10)°	β = 97.0090(10)°
	β = 68.8130(10)°	
	γ = 83.0100(10)°	
Volume /Å^3	1522.81(7)	3167.99(9)
Z, Calculated density /g.cm^{-3}	2, 1.522	4, 1.596
Absorption coefficient /mm^{-1}	5.117	5.019
F(000)	704	1504
Crystal size / mm	0.056 x 0.117 x 0.276	0.299 x 0.240 x 0.181
Theta range /°	3.06 to 25.50°	2.55 to 25.50°
Index range	$-13 \le h \le 13$,	$-13 \le h \le 13$,
	$-15 \le k \le 14$,	$-27 \le k \le 24$,
	$-15 \le l \le 14$	$-15 \le l \le 14$
Reflections collected	25655	30862
Independent reflections	5811 [$R_{(int)}$ = 0.0519]	5888 [$R_{(int)}$ = 0.0248]
Completeness to theta max.	99.7 %	99.9 %
Max. and min. transmission	0.7626 and 0.3325	0.3143 and 0.4652
Refinement method	Full-matrix	Full-matrix
	least-squares on F^2	least-squares on F^2
Data / restraints / parameters	5811/0/334	5888/0/322
Goodness-of-fit on F^2	0.951	1.066
Final *R* indices [*I*>2sigma(*I*)]	R_1 = 0.0348	R_1 = 0.0247
	wR_2 = 0.0809	wR_2 = 0.0621
R indices (all data)	R_1 = 0.0544,	R_1 = 0.0316
	wR_2 = 0.0850	wR_2 = 0.0640
Largest diff. peak and hole (e$^-$.Å^{-3})	0.406 and −0.553	0.965 and −0.724

Table 2 Important bond lengths/Å and bond angles/° for **1** and **2**

	Complex **1**	Complex **2**
Hg1-N1	2.510(5)	2.396(3)
Hg1-N2	2.594(5)	2.498(3)
Hg1-Cl1	2.399(2)	–
Hg1-Cl2	2.314(2)	–
Hg1-S1	–	2.533(9)
Hg1-S2	–	2.412(12)
C33-N3	–	1.152(5)
C34-N4	–	1.150(7)
C1-N1	1.261(8)	1.273(4)
C2-N2	1.275(8)	1.264(4)
C1-C2	1.519(10)	1.522(4)
N1-C13	1.448(9)	1.453(4)
N2-C19	1.417(9)	1.447(4)
N1-Hg1-N2	66.91(18)	69.89(8)
C1-N1-Hg1	111.8(5)	114.1(2)
C13-N1-Hg1	123.(4)	125.50(19)
C2-N2-C19	119.2(6)	119.6(3)
Cl1-Hg1-Cl2	141.93(8)	–
N1-Hg1-Cl1	89.42(14)	–
N1-Hg1-Cl2	128.05(15)	–
S1-Hg1-S2	–	122.45(5)
S1-Hg1-N1	–	101.63(7)
S1-Hg1-N2	–	93.44(6)
S1-C33-N3	–	178.5(4)
S2-C34-N4	–	176.6(5)

one sees that the symmetric stretch is displaced in both complexes, which is an indication of metal complexation at the diimine nitrogens atoms. Thiocyanate absorptions are also seen in the high frequency spectrum of **2**, at 2137(ν_{as}) and 2062(ν_s) cm^{-1}, respectively. Whereas the 2062 cm^{-1} absorption is invariant in both the free and in the complexed ligand, the absorption at 2137 cm^{-1} is indicative of bonding to the metal via the S atom, which increases the CN bond order. Indeed, the CN absorption in ionic thiocyanate, such as in K$^+$[NCS]$^-$, occurs at 2032 cm^{-1} [11]. Considering that this ionic compound has an average CN bond order between 3 and 2, due to resonance, an increase in the absorption value means that the CN bond force constant and hence the CN bond order of the complex is greater than that of the free ligand, i.e., the bond to the metal is likely to occur via the S atom. This spectral evidence is confirmed by the X-ray results. All other absorptions are listed in the experimental section.

Crystal data, details of data collection and structure refinement are listed in Table 1. Selected bond distances and angles of the complexes **1** and **2** are listed in Table 2.

In the crystal structure of **1**, the mercury atom is coordinated to two chloride ions and to the α-diimine in a bidentate manner. Thus, the mercury atom in **1** has a coordination number of four, with a distorted tetrahedral surrounding. The crystal structure of **2** shows the same characteristics of **1**, with the difference of having two thiocyanate ligands replacing the chlorides. Another feature shared by both complexes is the relative position of the substituents in the aromatic rings; in both the *tert*-butyl groups are *cis*, preserving the same configuration already seen in the crystal structure of the free ligand [9]. The crystal structures of **1** and **2** are shown in Figures 1 and 2, respectively.

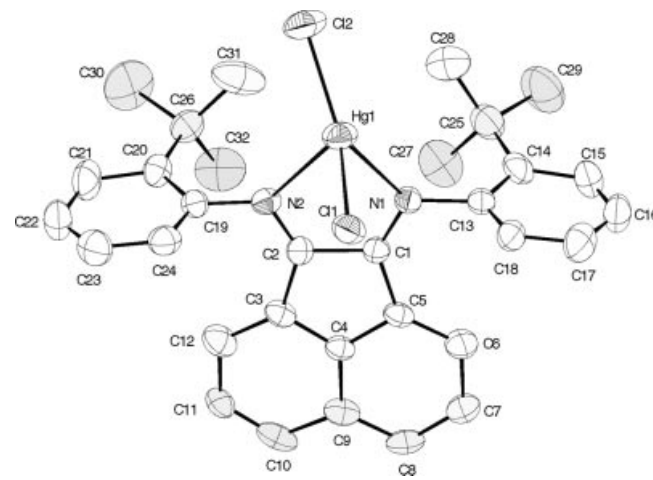

Figure 1 ORTEP [13] projection of complex bis[N-(2-t-butylphenyl)imine]acenaphthenedichloromercury(II) (**1**). Thermal ellipsoids in the level of 40 % of the probability. H atoms were omitted for better visualization.

The Hg1-N1 and Hg1-N2 bond lengths of **1**, 2.510(5) Å and 2.594(5) Å, respectively, are longer than the similar bond lengths of **2**, 2.396(3) Å and 2.498(3) Å, respectively. This difference can be assigned to a stronger coordination of the metal to the α-diimine in **2**. On the other hand, the N1-Hg1-N2 bite angles of 66.91(18)° and 69.89(8)°, for **1** and **2**, respectively, show no significant difference.

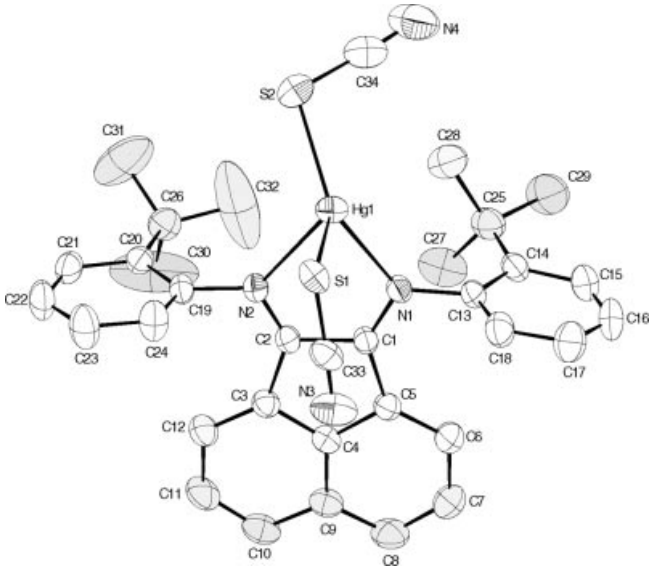

Figure 2 ORTEP [139 projection of complex bis[N-(2-t-butylphenyl)imine]acenaphthenebis(thiocyanate)mercury(II) (**2**). Thermal ellipsoids in the level of 40 % of the probability. H atoms were omitted for better visualization.

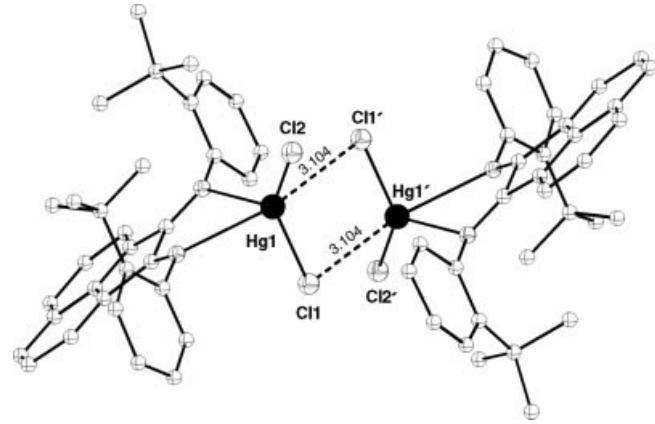

Figure 3 Dimeric structure [13] of **1**. Symmetry code for equivalent atoms, (′) = $-x$, $1-y$, $1-z$. H atoms were omitted for better visualization.

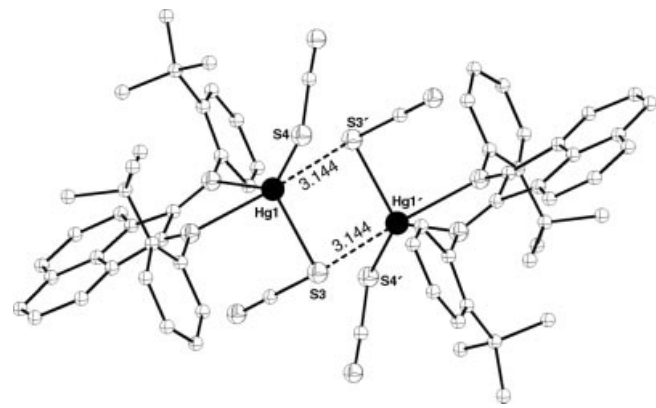

Figure 4 Dimeric structure [13] of **2**. Symmetry code for equivalent atoms, (′) = $-x$, $1-y$, $1-z$. H atoms were omitted for better visualization.

The bond lengths in **1**, 2.399(2) Å and 2.324(2) Å for Hg1-Cl1 and Hg1-Cl2, respectively, agree well with values found in the literature [8]. The bond lengths C-S and C-N of the thiocyanate group in **2** are also in agreement with the literature [12]. The bond lengths C33-N3 and C34-N4, of 1.152(5) Å and 1.150(7) Å, respectively, correspond to lengths more akin to a triple bond, which explains the higher CN stretching frequency observed in the i.r. spectrum, as discussed above. Selected geometric parameters for **1** and **2** are collected in Table 2 and conform to expected values.

The complexes form centrosymmetric dimers held together by weak Hg-Cl and Hg-S bonds, which can be visualized in Figures 3 and 4. In **1** the dimeric structure is built by the interaction of the Hg1 mercury atom of the asymmetric unit with the Cl1′ chloride ion of a neighbor molecule. Likewise, the Hg1′ atom interacts with the Cl1 chloride ion of the asymmetric unit. The two Hg-Cl distances are both 3.104(2) Å. It is noteworthy that the sum of the covalent radii of the atoms involved is lower than the sum of the van der Waals radii. [symmetry code (′) = $-x$, $1-y$, $1-z$]

The observed interactions for **2** also led to a dimeric structure with an inversion center, as shown in Figure 4. The structure confirms that the metal-ligand interaction takes place via the sulfur atoms, with an observed Hg-S distance of 3.144(2) Å, showing again the high affinity between mercury and sulfur, in agreement with the hard-soft acid-base concept.

Another feature shared by the structures of both **1** and **2** is a staggered Hg-containing five-membered ring in which there is a deviation from planarity. In **1** the dihedral angle amounts to 27.84(3)° between the fragments N1-C1-C2-N2 (r.m.s = 0.0086 Å) and N1-Hg1-N2. In **2** this deviation is 15.94(1)°, involving the homologous fragments (r.m.s = 0.0071 Å); this five-membered ring is thus more staggered in **1** than in **2**. Nevertheless, both angles are relatively high, and can be attributed to the presence of tert-butyl groups on the aromatic rings and to the intermolecular interactions in the dimeric structures.

Analysis of the supramolecular structure of **1** shows that a one-dimensional network is built along the *b*-axis as a consequence of the packing of the molecules by means of a stacking of the acenaphthene rings. The distance of the π-π interactions is 3.671(1) Å, in agreement with the literature [14]. Figure 5 shows the arrangement along the *b* crystallographic axis.

In **2**, the supramolecular arrangement shows that the crystal packing is achieved by non classical H-bonding [15]. These interactions were calculated using the Platon program [16] having C22 in the asymmetric unit as the H donor, and N4″ in a neighboring molecule as the H acceptor. The C22···N4″ distance is 3.457(2) Å, whereas the N4″···H22 distance is 2.579(2) Å. The C22-H22···N4″ angle

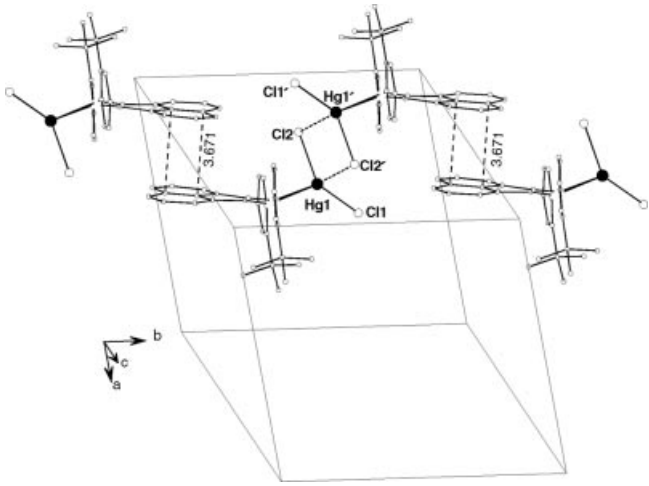

Figure 5 Packing [13] of **1** along the *b* axis. Symmetry for equivalent atoms (′) = $-x$, $1-y$, $1-z$. H atoms were omitted for better visualization.

is 156.72(1)°. When a dimer occurs, this intermolecular interaction can be generated by symmetry along both the b as well as the c crystallographic axis, as shown in Figure 6. [Symmetry code (″) = $-0.5-x$, $0.5+y$, $2-z$]

Thus the dimer will present a total of 4 interactions, all of them with the same structural parameters.

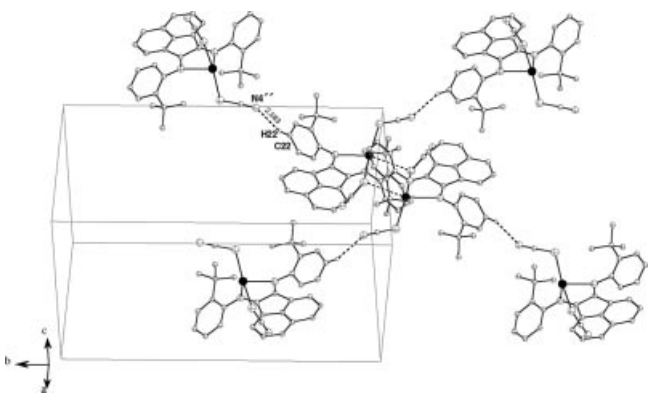

Figure 6 Packing [13] of **2** along the *b* and *c* axis. Symmetry code for non classical hydrogen bonds, (″) = $-0.5-x$, $0.5+y$, $2-z$. Non essential H atoms were omitted for better visualization.

The set of data shown is an evidence of how the one pot reaction technique was essential in order to obtain the complexes described in this work, and led to good chemical yields. An analysis of the i.r. spectra gave a good indication of this success and of the types of bonding in the complexes, from the observation of the appearance of CN imine stretching modes and from their frequencies. Structural analysis by X-ray diffraction led to the establishment of their crystal structures as well as to the supramolecular arrangement formed by intermolecular interactions due to π-π interactions and non classical H-bonding, respectively.

Experimental Section

Melting points were determined, without correction, from a Quimi Q-40M apparatus. Elemental analyses were obtained from a 2400 Perkin-Elmer instrument, using a PE AD-4 balance. I.R. spectra were collected from a Magna-FTIR Nicolet spectrometer, and ^{1}HNMR spectra were run at room temperature using a 200 MHz Bruker instrument.

X-ray diffraction data were collected at 295 K from a *Bruker AP-EXII-CCD* [17] diffractometer with graphite monochromatized Mo K_α radiation. Cell parameters of complexes **1** and **2** were obtained and refined using the *SAINT* [17] program. Absorption correction was made with the *SADABS* [17] program. Data collection analysis revealed for **1** and **2** a ***triclinic P*$\bar{1}$** and a ***monoclinic P*2$_1$*/c*** space group, respectively. The structures were solved by Direct Methods using the *SHELXS*-97 [18] program. Atom positions were refined using the SHELXL-97 [19] program with anisotropic displacement parameters for all non-H atoms. H atoms were included in idealized calculated positions and refined riding on their respective C atoms. Aromatic carbons were refined with U_{iso}(H) = 1.2 *Ueq* Csp^2 and *tert*-butyl group with U_{iso}(H) = 1.5 *Ueq* Csp^3. X-ray data are listed in Table 1. The solution and refinement of **1** suggested the presence of two markedly disordered water molecules as crystallization solvates. The hydrogen atom coordinates corresponding to those water molecules could not be localized experimentally in the Fourier map. In view of this we opted for utilizing the SQUEEZE [20] tool contained in the WinGX [20] package, in order to exclude any electronic density contributions relative to the disordered water molecules. This procedure is in accordance with the elemental analysis of the complex, confirming a species free from any cristallization solvate. This is validated insofar as the water molecules do not contribute to the supramolecular arrangement under discussion. The C30, C31 and C32 atoms exhibit disorder effects, which were shown as a result of the anisotropic refinement. Their U_{eq} values are C30, 92(2); C31, 107(3); C32, 94(2), respectively.

CCDC 670143 & 670144 contains the supplementary crystallographic data for this paper. These data can be obtained free of charge from The Cambridge Crystallographic Data Centre via www.ccdc.cam.ac.uk/data request/cif.

Preparation of bis[N-(2-t-butylphenyl)imine]acenaphthenedichloromercury(II), (1) and bis[N-(2-t-butylphenyl)imine]acenaphthenebis(thiocyanate)mercury(II), (2)

The syntheses of both complexes were carried out using the technique known as "one pot reaction" [7]. However, in the cases of complexes (**1**) and (**2**) the preparations were modified in relation to those in the literature, according to which all materials are mixed together at once in the reaction flask. In our case, the organic starting materials (acenaphthenequinone, 2-*t*-butylaniline and HOAc as catalyst) were initially dissolved in MeOH, and only after some time the metal salt was added, as described below. Scheme 1 shows the corresponding equation.

0.547 g (3 mmol) of acenaphthenequinone and 0.935 mL (6 mmol) of 2-*t*-butylaniline were added to a 100 mL round bottom flask containing 30 mL of MeOH and 5 drops of glacial HOAc. The flask was connected to a Liebig condenser and heated under stirring. The temperature was kept 20 °C above the boiling point of the solvent. The color of the mixture changed from yellow to dark

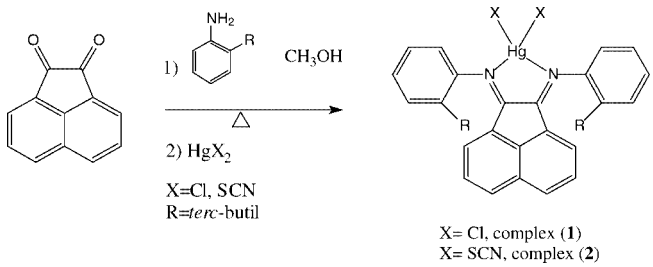

Scheme 1 Equation for the preparation of **1** and **2**.

red. After 1h30m, heating was interrupted and the mixture cooled to room temperature. At this point 3 mmol of the Hg^{II} salt was added (chloride or thiocyanate, respectively) and an orange precipitate was immediately formed. The mixture was then kept under reflux for 2 more hours. The solid was filtered off and washed with 25 mL of cold MeOH. It was dried *in vacuo* and weighed, giving 1.61 g (75 %) in the case of **1** and 1.76 g (81 %) in the case of **2**. Both solids were recrystallized from $CHCl_3$, and after a few days bright orange crystals formed. These were used in m.p. determinations, elemental analyses, i.r. and ^{1}HNMR spectroscopy, and X ray crystallography.

Properties of **1**. Yield, 75 %; m.p. 264−266 °C; C,H,N analysis: calcd. for 715.65 $gmol^{-1}$, C, 53.7; H, 4.47; N, 3.91 %; found, C, 53.4; H, 4.2; N, 3.8 %.

IR spectroscopy (CsI pellet and nujol film between polyethylene sheets), cm^{-1}: 3097m, 3057m, 2992s, 2960s, 2098m, 2868m, 1667m, 1626s, 1587s, 1568w, 1481s, 1434s, 1420m, 1363m, 1282s, 1286m, 1239m, 1227m, 1207m, 1108m, 1082m, 1050s, 936m, 833s, 780s, 760s, 752s, 565m, 539s, 521s, 493m, 453m, 408m and 311s. **^{1}HNMR** (200 MHz in $CDCl_3$, δ(ppm) relative to TMS): 1.37 (s, 18H, tert-butyl), 6.62−8.45 (aromatic hydrogens)

Properties of **2**. Yield, 81 %; m.p. 279−280 °C; C,H,N analysis: calcd. for 760.65 $gmol^{-1}$, C, 53.6; H, 4.2; N, 7.4 %; found, C, 53.3; H, 4.1; N, 7.2 %.

IR spectroscopy (CsI pellet and nujol film between polyethylene sheets), cm^{-1}: 3060m, 2989s, 2967s, 2907m, 2871m, 2137vs, 2126s, 2062m, 2063m, 1666m, 1626s, 1600m, 1588s, 1482s, 1437s, 1363m, 1283m, 1240m, 1203m, 1109m, 1081m, 1050m, 938m, 833m, 779s, 758s, 563m, 539s, 491m, 452s, 417m, 407s,277s, 246m, 119m and 82m. **^{1}HNMR** (200 MHz in $CDCl_3$, δ(ppm) relative to TMS: 1.42 (s, 18H, tert-butyl), 6.63−8.56 (aromatic hydrogens)

Acknowledgements. The authors are grateful to their sponsors, CNPq and CAPES.

References

[1] M. Brookhart, A. F. Volpe, D. M. Lincoln, I. T. Hovarth, J. M. Millar, *J. Am. Chem. Soc*. **1990**, *112*, 5634.
[2] F. C. Rix, M. Brookhart, *J. Am. Chem. Soc.* **1995**, *117*, 1137−1138.
[3] M. J. Tanner, M. Brookhart, J. M. DeSimone, *J. Am. Chem. Soc.* **1997**, *119*, 7617−7618.
[4] H. T. Dieck, J. Dietrich, *Chem. Ber*. **1984**, *117*, 694.
[5] A. Paulovicova, U. El-Ayaan, K. Shibayama, T. Morita, Y. Fukuda, *Eur. J. Inorg. Chem*. **2001**, *10*, 2641.
[6] R. Van Asselt, C. J. Elsevier, W. J. J. Smeets, A. L. Spek, R. Benedix, *Rec. Trav. Chim. Pays-Bas* **1994**, *113*, 88.
[7] M. D. Rausch, J. C. W. Chien, J. S. Wood, R. J. Maldanis, *J. Organomet. Chem.* **2002**, *645*, 158−167.
[8] U. El-Ayaan, *Monatsh. Chem.* **2004**, *135*, 919−925.
[9] L. C. Ferreira, C. A. L. Filgueiras, M. Hörner, L. C. Visentin, J. Bordinhão, *Acta Crystallogr.* **2007**, *E63*, o3427.
[10] John Dyer, *Applications of absortion spectroscopy of organic compounds*, 3rd ed., Ed. Edgard Blücher, 1969, pps 36−41.
[11] K. Nakamoto, *Infrared and Raman Spectra of Inorganic and Coordination Compounds*, 3rd ed., Ed. Wiley and Sons, 1963, pps 270−271.
[12] R. Kapoor, A. Kataria, A. Pathak, *Polyhedron* **2005**, *24*, 1221−1231.
[13] L. J. Farrugia, *ORTEP-3* for Windows, *J. Appl. Cryst*. **1997**, *30*, 565.
[14] U. Mukhopadhyay, D. Choquesillo-Lazarte, J. Niclós-Gutierrez, I. Bernal, *CrystEngComm* **2004**, *6(102)*, 627−632.
[15] G. A. Jeffrey, H. Maluszynska, J. Mitra, *Int. J. Biol. Macromol*. **1985**, *7*, 336−348.
[16] A. L. Spek, *PLATON* program, *J. Appl. Cryst*. **2003**, *36*, 7.
[17] Bruker AXS Inc., Madison, Wisconsin, USA, © 2005, *SAINT* (Version 7.06A), *SADABS* (Version 2.10).
[18] G. M. Sheldrick, *SHELXS97*, Program for Crystal Structure solution. 1997, University of Göttingen, Germany.
[19] G. M. Sheldrick, *SHELXL97*, Program for crystal structure Refinement, 1997, University of Göttingen, Germany.
[20] L. J. Farrugia, *WinGX* program, *J. Appl. Cryst*. **1999**, *32*.

